Photodynamics of Nickel Porphyrins in Noncoordinating Solvents: Characterization of d-d Excited States Using Transient Raman Spectroscopy

ARTICLE *in* THE JOURNAL OF PHYSICAL CHEMISTRY · JANUARY 1988

Impact Factor: 2.78 · DOI: 10.1021/j100313a014

3 AUTHORS, INCLUDING:

John A Shelnutt
University of Georgia
265 PUBLICATIONS **8,720** CITATIONS

Photodynamics of Nickel Porphyrins in Noncoordinating Solvents: Characterization of d–d Excited States Using Transient Raman Spectroscopy†

E. W. Findsen,*‡ J. A. Shelnutt,§ and M. R. Ondrias‡

Department of Chemistry, University of New Mexico, Albuquerque, New Mexico 87131, and Sandia National Laboratories, Albuquerque, New Mexico 87185 *(Received: April 24, 1987)*

The photodynamic behavior of several nickel porphyrins in noncoordinating solvents was investigated with absorption and transient Raman spectroscopies. A recent transient absorption study of nickel porphyrins, in noncoordinating solvents, by Kim et al. (*Chem. Phys.* **1983**, *75*, 305) proposed that, upon photoexcitation from the ground 4-coordinate state ($^1A_{1g}$), the excited-state decay path traverses a state in which the metal is in an electronic state (designated here as $^*B_{1g}$) similar to that observed for the metal in coordinating solvent systems ($^3B_{1g}$). This excited state involves the net promotion of one of the two nickel electrons in the d_{z^2} orbital into the empty $d_{x^2-y^2}$ orbital. While the lifetime of the $^*B_{1g}$ state has been estimated to be ~250 ps, it can be observed by using ~10-ns-wide laser pulses under appropriate experimental conditions. Simple calculations demonstrate the effect of state lifetimes upon the population of the excited-state species within the nanosecond laser pulse. The $^*B_{1g}$ state is reversibly formed for several nickel porphyrins in all noncoordinating solvents used. This state is identified in transient Raman spectra by shifts in several lines. Three of these lines are sensitive to changes in the core size of the porphyrin and indicate expansion of the porphyrin core to accommodate the increased in-plane electron density caused by the electron promotion on the metal. Detailed examination of one nickel porphyrin, NiPPDME, indicates a dependence of the $^*B_{1g}$ state's vibrational characteristics upon the solvent environment and implies that the porphyrin a_{2u} orbital is very sensitive to solvent environment. Absorption studies indicate that while both the a_{1u} and a_{2u} orbitals can be influenced by the solvent environment, the a_{2u} orbital is the most affected.

Introduction

Metalloporphyrins serve nature in a variety of ways. In the biochemical world, they are the active sites of proteins whose functions range from oxygen transport and storage (hemoglobin, myoglobin) to electron transfer (cytochrome *c*, cytochrome oxidase) to energy conversion (chlorophyll). Recently, a nickel-containing tetrapyrrole was found to play a catalytic role in the biosynthesis of methane by methanogenic bacteria.[1] Additionally, porphyrins have proven to be efficient sensitizers and catalysts in a number of inorganic chemical and photochemical systems. The mechanisms by which metalloporphyrins perform such diverse functions continue to be the focus of extensive spectroscopic investigation. It is particularly important that the excited-state properties of these complex molecules be understood in order to make full use of the unique photochemical abilities of metalloporphyrins.

The study of the photodynamics of metalloporphyrins has, in the past, been the domain of workers using transient absorption techniques. The formation of an excited-state species in a nickel porphyrin in a noncoordinating solvent was first proposed by Cheung et al.,[2] but no attempt was made to characterize this species. Later studies using transient absorption spectroscopy characterized the decay mechanism of nickel porphyrins in both coordinating and noncoordinating solvents.[3-7] The most detailed studies in this area are those of Kim et al.[3,4] Their reports present a complete picture of the decay paths and the lifetime of the states involved. Building on this extensive background, we can, using transient Raman spectroscopy, observe the effects of the excited electronic state of the metal on the vibrational properties of the porphyrin macrocycle. Recently, transient Raman spectroscopy has been used to characterize the vibrational response of several nickel porphyrins to photoinduced deligation.[8,9] These studies clearly demonstrated the applicability of transient Raman spectroscopy to this problem as well as the wealth of structural information this technique can provide. While previous studies concentrated upon the photodynamics of nickel porphyrins in coordinating solvents, some preliminary results of experiments with nickel protoporphyrin in two noncoordinating solvent systems were also presented. This report expands upon those earlier studies providing a detailed analysis of the structural characteristics of the excited states of nickel porphyrins in noncoordinating solvents.

Experimental Section

Nickel protoporphyrin IX (NiPP), nickel protoporphyrin IX dimethyl ester (NiPPDME), and nickel octaethylporphyrin (NiOEP) were obtained from Porphyrin Products (Logan UT) and were used without further purification. Organic solvents were of spectral or AR grade (Aldrich, Fisher) and were used without further purification. Cetyltrimethylammonium bromide (CTAB; Sigma Chemical), and sodium dodecyl sulfate (SDS; United States Biochemical Co.) were also used as received. Samples were contained in either a quartz EPR tube (Wilmad) or a standard quartz cuvette. All spectra were obtained at ambient temperature (20–25 °C). Since no sample degradation was observed in aerobic vs anaerobic samples, deoxygenation of the samples was not routinely performed. Sample integrity was monitored with UV–visible spectroscopy.

Transient Raman data were obtained by using an instrument described in detail elsewhere.[10] Soret excitation was provided by a Molectron N_2-pumped dye laser. Visible excitation was provided by a Quanta-Ray DCR-II Nd:YAG laser using the second harmonic (532 nm) of the fundamental. A backscattering geometry was utilized, and the scattered radiation was focused into a SPEX Industries 1403 scanning double monochromator. The Raman scattered radiation was detected by a photomultiplier in a cooled housing. The photomultiplier output was fed into an EG&G boxcar (162/165), whose output was then directed into a SPEX Industries Datamate controller, which controlled the

† This work performed at the University of New Mexico and Sandia National Laboratories, Albuquerque, New Mexico.
‡ University of New Mexico.
§ Sandia National Laboratories.

(1) Wolfe, R. S. *Trends Biochem. Sci.* **1985**, *10*, 396–399.
(2) Cheung, L. D.; Yu, N.-T.; Felton, R. H. *Chem. Phys. Lett.* **1978**, *55*, 527–530.
(3) Kim, D.-H.; Kirmaier, C.; Holten, D. *Chem. Phys.* **1983**, *75*, 305–322.
(4) Kim, D.-H.; Holten, D. *Chem. Phys. Lett.* **1983**, *98*, 584.
(5) Holten, D.; Gouterman, M. In *Proceedings of the Symposium on Optical Properties and Structures of Tetrapyrrole*; Konstanz, Springer-Verlag: New York, 1984.
(6) Kobayashi, T.; Straub, K.; Rentzpeis, P. M. *Photochem. Photobiol.* **1979**, *29*, 925.
(7) Chirvonyi, V. S.; Dzhagarov, B. M.; Timinskii, Y. V.; Gurinovich, G. P. *Chem. Phys. Lett.* **1980**, *70*, 79.
(8) Kim, D.-H.; Spiro, T. G. *J. Am. Chem. Soc.* **1986**, *108*, 2099.
(9) (a) Findsen, E. W.; Shelnutt, J. A.; Friedman, J. M.; Ondrias, M. R. *Chem. Phys. Lett.* **1986**, *126*, 465–471. (b) Findsen, E. W.; Shelnutt, J. A.; Ondrias, M. R. *J. Am. Chem. Soc.* **1986**, *108*, 4009–4017.
(10) Findsen, E. W. Doctoral Disseration, University of New Mexico, 1986.

0022-3654/88/2092-0307$01.50/0

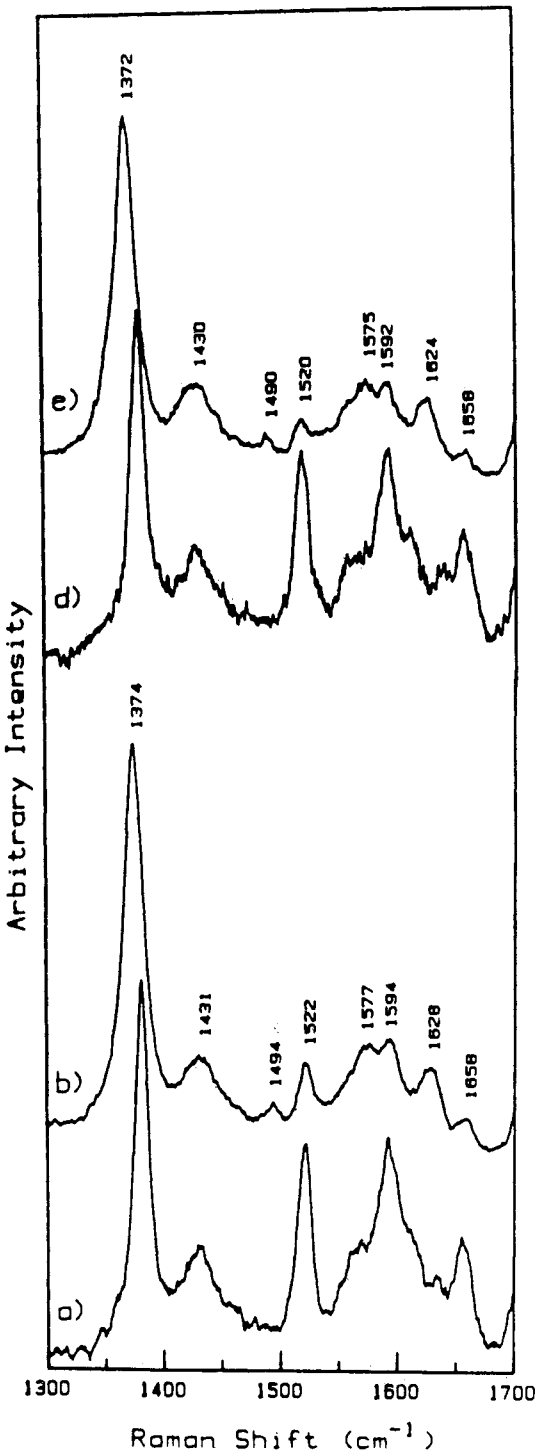

Figure 1. Raman spectra of the 4-coordinate equilibrium ground-state species (a and d) of NiPP and NiPPDME in 10% H_2O/acetone. Spectra b and e are representative of those obtained using high photon density. The new peaks appearing in the spectra are due to the $^*B_{1g}$ state formed under these conditions. The excitation wavelength used, 406 nm, was chosen to correspond to the absorption maximum of the 4-coordinate equilibrium species, thus maximizing the production of the excited-state species. The experimental parameters, such as the laser beam focus and sample concentration, were identical for all spectra (in a given series). The incident laser power was controlled by the use of neutral density filters.

monochromator and stored the data during acquisition. The data were then transferred to an Apple computer for storage and graphic manipulation.[11] All spectra are the unsmoothed sum of several scans.

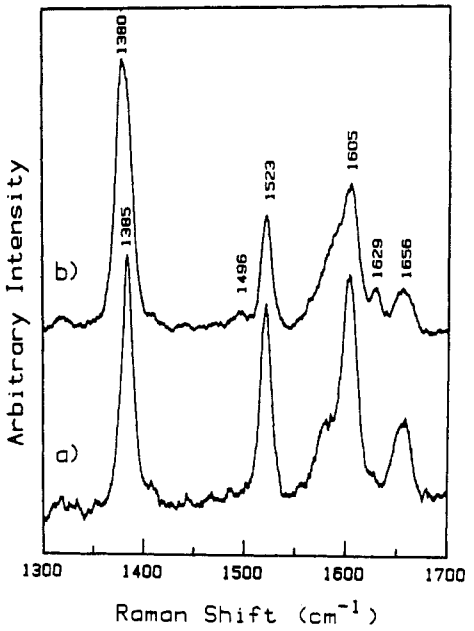

Figure 2. Transient resonance Raman spectra of NiOEP in toluene using 406 nm excitation. Spectrum a was obtained at low photon densities with a very defocused cylindrical lens (see Experimental Section). Spectrum b was obtained at high photon densities with a sharply focused spherical lens. A solvent vibrational mode may contribute to the intensity of the region between ~1550 and 1660 cm^{-1}. The influence of this interference upon porphyrin line positions is minimal due to the relatively high porphyrin concentration (~50 μM).

Control of photon densities at the sample was necessary to obtain spectra of the ground- and excited-state species. Laser power densities were controlled in one of three ways or in combination: (1) use of either a spherical or cylindrical lens to image the laser beam onto the sample; (2) the actual focus of the imaging optic; (3) use of neutral density filters. We estimate the power densities at the sample, for Soret excitation, to be in the range of 10 mJ/cm^2 (for low-power studies) to 400 mJ/cm^2 (for high-power studies).

Results

The reversible formation of an excited-state species at high power is clearly demonstrated in Figures 1–3. A spectrum of the 4-coordinate ground-state species taken at low power is shown in Figure 1a. This spectrum is typical of those observed for nickel porphyrins in noncoordinating solvents. Nickel protoporphyrin in H_2O/acetone exhibits values of 1652, 1592, 1522, and 1382 cm^{-1} for vibrations that are assigned to $^4\nu_{10}$, $^4\nu_2$, $^4\nu_3$, and $^4\nu_4$,[25] respectively. These values are characteristic of 4-coordinate species.[8,9] The excited-state species has modes at 1628, 1577, 1494, and 1374 cm^{-1} which are assigned to $^*\nu_{10}$, $^*\nu_2$, $^*\nu_3$, and $^*\nu_4$, respectively. These frequencies are assigned by analogy to modes observed for NiPP in coordinating solvents and NiPP incorporated in hemoglobin and myoglobin[12] but are distinct from them. Table I presents the results of power-dependence studies on NiPP, NiPPDME, and NiOEP, in a number of noncoordinating solvent systems. No significant frequency dependence on the porphyrin peripheral substituents was observed (compare, for instance, the spectral data of NiPP and NiPPDME in the same solvents, as well as the results of studies of NiOEP).

Figure 1 presents spectra of NiPPDME and NiPP in 10% H_2O/acetone. Figure 2 presents spectra of NiOEP in toluene obtained with low and high photon densities. Spectra of NiOEP in dichloromethane were similar to those obtained in toluene but are not presented. Figure 3 presents spectra of NiPP in CTAB micelles obtained with 532-nm excitation at several power levels. As the power increases, the intensities of several new modes, which

(11) Findsen, E. W.; Ondrias, M. R. *Photochem. Photobiol.* **1986**, *43*, 229–232.

(12) Shelnutt, J. A.; Alston, K.; Ho, J.-Y.; Yu, N.-T.; Yamamoto, T.; Rifkind, J. M. *Biochemistry* **1986**, *25*, 620–626.

TABLE I: Raman Modes Observed in Noncoordinating Solvents[a]

solvent	mode							
	$^4\nu_4$	$^4\nu_3$	$^4\nu_2$	$^4\nu_{10}$	$^*\nu_4$	$^*\nu_3$	$^*\nu_2$	$^*\nu_{10}$
				Ni(PP)				
H_2O/acetone	1382	1522	1592	1656	1374	1494	1577	1628
SDS	1384	1523	1597	1662	1376	1495	1577	1632
CTAB	1383	1524	1596	1660	1374	1492	1572	1627
NaOH/MeOH	1386	1524	1598	1657	1378			1626
DMSO	1385	1524	1594	1654	1374	1490	1575	1624
				Ni(PPDME)				
H_2O/acetone	1381	1521	1593	1656	1372	1490	1575	1624
toluene	1383	1522	1598	1658	1377	1497	1574	1632
benzene	1382	1521	1592	1657	1375	1495	NR	1629
Br-benzene	1382	1521	1596	1658	1374	1493	1578	1626
CHI_3	1382	1522	1594	1657	1373	1494	1583	1626
CH_2Cl_2	1381	1522	1601	1657	1372	1493e	1583	1624
acetone	1382	1520	1593	1655	1376	1490	1573	1628
DMSO	1382	1522	1593	1657	1373	1490	1573	1626
				Ni(OEP)				
toluene	1385	1522	1582e	1657	1380	1496	NR	1629
CH_2Cl_2	1387	1524	1578e	1658	1381	1498e	1580e	1631e

[a] Asterisk indicates excited-state species. Accuracies are assumed to be ±1 cm^{-1}. The lowercase e beside some values indicates that this position is estimated because of the presence of interfering bands. NR indicates not resolved.

TABLE II: Calculated Core Sizes (Å) of Equilibrium and Excited-State Nickel Porphyrins[a]

solvent	$E_T(30)$	ν_2	ν_3	ν_{10}	$^*\nu_2$	$^*\nu_3$	$^*\nu_{10}$
			Ni(PP)				
pyrrolidine(6)	NA	2.015	2.039	2.027			
pyrrolidine(4)	NA	1.951	1.957	1.954			
H_2O/acetone	NA	1.951	1.954	1.954	1.994	2.017	2.011
SDS	NA	1.953	1.957	1.95	2.007	2.021	2.014
CTAB	NA	1.94	1.949	1.948	1.994	2.015	2.004
NaOH/MeOH	NA	1.948	1.952	1.963	NR	NR	2.017
DMSO	45	1.956	1.958	1.958	1.999	2.021	2.02
			Ni(PPDME)				
piperidine(6)	35.5	2.017	2.024	2.027			
piperidine	35.5	1.948	1.954	1.958			
pyrrolidine(6)	NA	2.016	2.03	2.029			
pyrrolidone		1.951	1.957	1.958			
H_2O/acetone	NA	1.955	1.959	1.954	1.999	2.027	2.02
toluene	33.9	1.94	1.954	1.954	2.002	2.01	2.004
benzene	34.5	1.956	1.957	1.956	NR	2.015	2.01
Br-benzene	37.5	1.946	1.957	1.954	1.992	2.019	2.016
$CHCl_3$	39.1	1.951	1.954	1.956	1.979	2.017	2.016
CH_2Cl_2	41.1	1.933	1.954	1.956	1.979	2.019	2.02
acetone	42.2	1.953	1.959	1.96	2.004	2.026	2.012
DMSO	45	1.953	1.954	1.956	2.004	2.025	2.016
			Ni(OEP)				
toluene	33.9	NR	1.952	1.958	NR	2.012	2.01
CH_2Cl_2	41.1	NR	1.95	1.954	NR	2.008	2.006

[a] Core sizes calculated using the observed empirical correlations between given mode frequencies and core size.[18,19] All ground-state species are 4-coordinate except those denoted as 6-coordinate by 6. In coordinating solvents, an equilibrium between 4- and 6-coordinate species exists and values for both ground-state species are given. In these cases, the 4-coordinate species is a minor component, making observation of its transient species impossible. Abbreviations: NR, not resolved; NA, not available.

we ascribe to the excited-state species, increase.

The dependence of the excited state upon solvent environment was explored by examining the behavior of the excited state of NiPPDME in a number of noncoordinating solvents. A systematic dependence upon solvent $E_T(30)$ (defined below) was observed for the positions of $^*\nu_3$, $^*\nu_{10}$, and $^*\nu_4$. The range of solvents used in the Raman study was limited by the solubility of NiPPDME in these solvents. These dependencies (or lack thereof in the case of $^*\nu_2$) are demonstrated in the plots of Figure 4 as well as in Tables I and II.

The absorption spectra of NiPPDME in the same series of noncoordinating solvents were also recorded. Spectral parameters were plotted against several solvent parameters, such as dipole moment, dielectric, and $E_T(30)$.[13] The $E_T(30)$ parameter is based upon the wavelength of a charge-transfer band of a pyridinium *N*-phenoxide betaine dye as a function of the solvent and thus reflects the combined effects of the dipolar and inductive properties of the solvent upon the dye's frontier molecular orbitals.[13] The dye has a nitrogen conjugated with a π electron system. This parameter yielded better fit to the data the than other solvent parameters. Moreover, Figure 5 clearly depicts a trend that indicates a specific electronic response by the porphyrin to the solvent environment. A correlated response to solvent $E_T(30)$ was found for the average energy of the B and Q (Soret and α) bands, the difference between the energy of these two bands, and the intensity ratio of the α-β bands. The average energy of the B and Q bands corresponds to the parameter A'_{1g} of the four-orbital model of Gouterman.[14] The energy difference between the B

(13) Reichardt, C. In *Solvent Effects in Organic Chemistry*; Verlag Chemie: Weinheim, 1978.

(14) Gouterman, M. In *The Porphyrins*; Dolphin, D., Ed.; Academic: New York, 1977; Vol. III, pp 1-165.

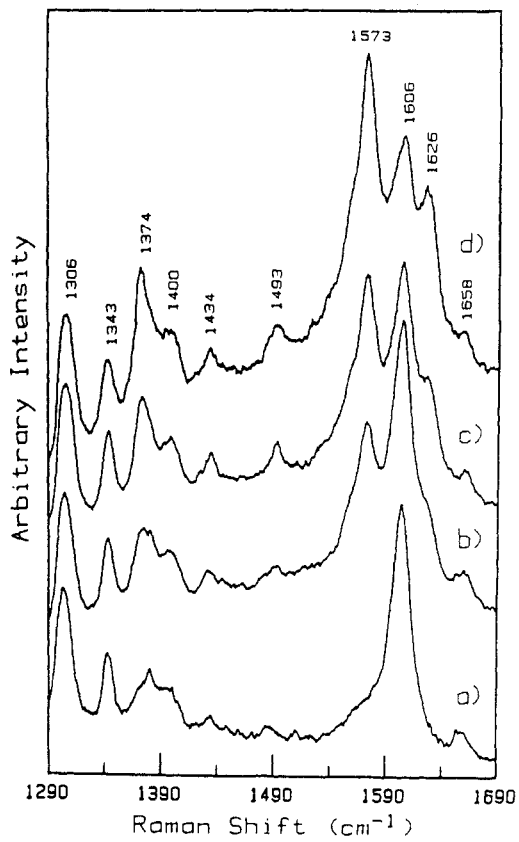

Figure 3. Transient Raman spectra of NiPP in CTAB micelles (0.1 M NaOH) using 532 nm excitation. All spectra were obtained under identical experimental conditions with the exception of the incident laser power. The incident laser power was controlled by the use of calibrated neutral density filters. Spectra were obtained in an alternating sequence of higher and lower laser powers in order to ascertain that all spectral changes were reversible. Some chlorin formation was observed (by absorption spectroscopy) after the highest power spectra were obtained, but the amount formed is estimated to be less than 10% and was not resonantly enhanced. Laser energies used to obtain the spectra: (a) ~0.5, (b) ~1.3, (c) ~2.5, and (d) ~4.8 mJ/pulse.

and Q bands is related to A_{1g} and A''_{1g} parameters of the same model. The application of the four-orbital model to these data will be discussed below.

In the course of these spectroscopic determinations, three solvents were determined to induce NiPPDME spectral behavior that did not follow one or more of the correlations described above. One solvent in particular, benzyl alcohol, failed all correlations. In the case of benzyl alcohol, if the $E_T(30)$ value of the parent molecule (toluene) is used in all of the plots presented above, the NiPPDME spectral values fall very close to the best fit line through the data points. This suggests that the aromatic properties of benzyl alcohol dominate the properties of the OH group for interaction with the porphyrin π system. Methanol and ethanol appear to fit all the correlations except for the intensity of the α–β ratio vs $E_T(30)$. This behavior appears to be common to solvents with $E_T(30)$ values greater than ~47. In this study, the anomalous solvents are all alcohols. They appear to form a separate correlation for the plot of α–β ratio vs $E_T(30)$ (see Figure 5).

Discussion

The characterization of the excited-state species serving as both the transition state for ligand binding and the "bottleneck" state for deactivation of electronically excited Ni–porphyrins is vital for a complete understanding of the complex photodynamic behavior of these molecules. Transient absorption spectroscopy has proven to be a very useful technique in the pursuit of this knowledge. However, transient absorption spectroscopy directly probes the electronic changes in the system, yielding only indirect information on the geometric response of the molecule to the

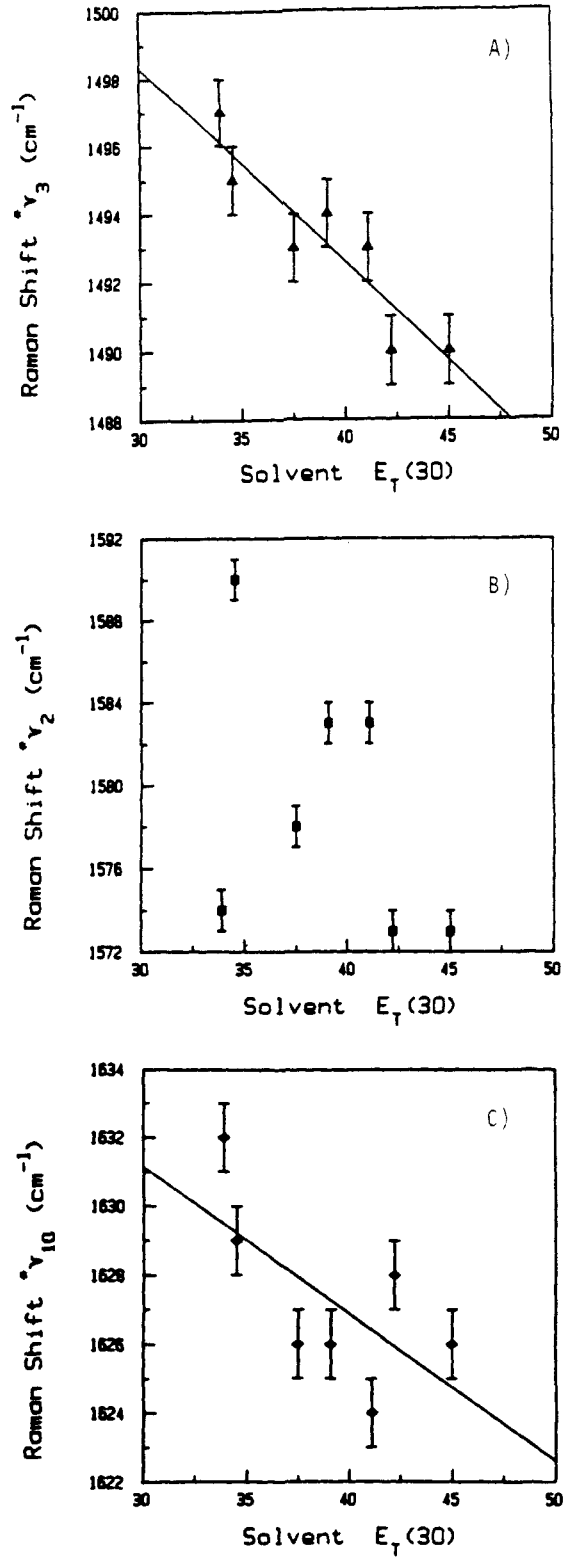

Figure 4. Relative response of several core size sensitive Raman lines to solvent $E_T(30)$ (see text). As can be seen, ν_3 and ν_{10} (graphs A and C) appear to correlate with this solvent parameter while ν_2 (graph B) does not. Error bars denote estimated accuracy of Raman line position (±1 cm^{-1}). The lines are a linear least-squares fit to the data in each panel.

electronic changes. Transient Raman spectroscopy, however, provides very detailed structural information about the properties of the molecular excited state via the vibrational response of the molecule.

Nickel Porphyrin Photodynamics. Nickel(II) porphyrins have eight metal d electrons, six of which fill the d_{xy}, d_{xz}, and d_{yz} orbitals. The other two electrons change their orbital occupation depending on the ligation state of the system. For 4-coordinate nickel porphyrins, both electrons reside in the d_{z^2} orbital, which is

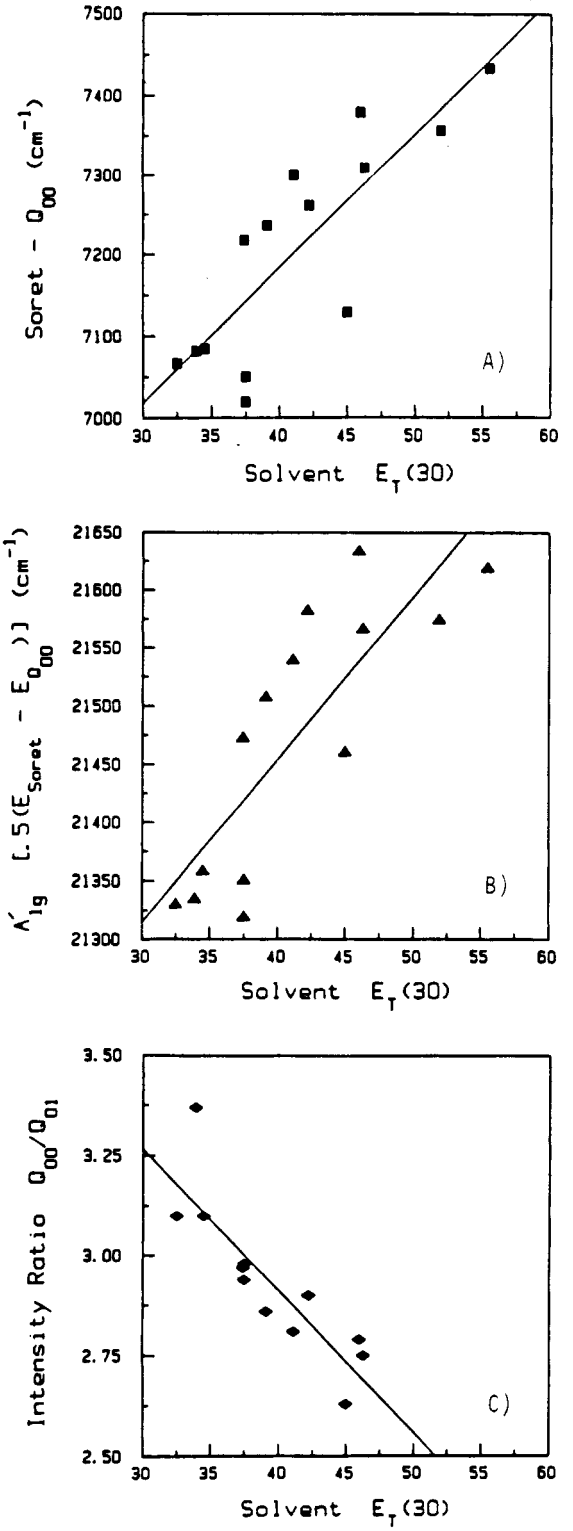

Figure 5. Sensitivity of absorption spectral parameters to solvent properties. Graph A demonstrates the response of the splitting of the B and Q bands to solvent E_T(30). Graph B portrays the response of the average energy of the B and Q bands, while graph C depicts the behavior of the ratio of the intensity of the porphyrin α–β bands to solvent E_T(30). The lines in each panel of the figure are the result of a linear least-squares fit to the data. Error bars are not present for clarity.

designated, by using group theoretical notation, the $^1A_{1g}$ state. In coordinating solvent systems, the two electrons each occupy different orbitals, namely, the $d_{x^2-y^2}$ orbitals. This state bears the designation of either $^3B_{1g}$ or $^1B_{1g}$, depending on the spin pairing of the two electrons. Theoretical calculations by Ake and Gouterman[15] have determined the relative energy level spacing for 4- and 5-coordinate nickel porphyrin systems.

The lifetimes of excited states in the decay path of several nickel porphyrin systems have been determined with transient absorption spectroscopy.[3-7] The studies by Kim et al.[3,4] present the most complete picture of the decay paths of nickel porphyrins in both coordinating and noncoordinating solvents and indicate that the porphyrin π–π^* excited states decay within a few picoseconds of excitation to a metal-centered, metastable excited state. For nickel porphyrins that have the $^1A_{1g}$ state as their ground state, the metal-centered excited states were found to have the following lifetimes and a decay path

$$^1A_{1g} \rightarrow \phi^* \quad (\sim ps)$$

$$\phi^* \rightarrow {}^*B_{1g} \quad (\sim 15\ ps)$$

$${}^*B_{1g} \rightarrow {}^1A_{1g} \quad (\sim 250\ ps)$$

where ϕ represents porphyrin-centered excited states.

In 4-coordinate nickel porphyrins, singlet and triplet B_{1g} states are higher in energy than the $^1A_{1g}$ state. This is reasonable since the $d_{x^2-y^2}$ orbital points directly at the pyrrole nitrogens of the porphyrin macrocycle. Normally, the occupation of this orbital is favored only when nitrogenous σ-donating molecules are available for ligation at the axial sites of the porphyrin, raising the energy of the d_{z^2} orbital and therefore the $^1A_{1g}$ state. However, the results of transient absorption experiments and theoretical calculations indicate that, upon photoexcitation, a long-lived (~250 ps) B_{1g} state is the lowest lying intermediate in the excited-state decay pathway.

In this path, there is no state with a lifetime in the nanosecond time scale, and one would naively assume that the observation of the $^*B_{1g}$ state with a lifetime of ~250 ps would not be possible using a 20-ns-wide laser pulse. However, the 250-ps lifetime of the state is long enough (relative to the 15-ps half-life for formation) to permit the buildup of a significant concentration of excited-state species within the several-nanosecond-wide laser pulse.

In previous reports, we presented the results of transient Raman studies in the photodissociation behavior of several nickel porphyrins in coordinating solvents.[8,9] In these systems, the ground state of the metalloporphyrin is $^3B_{1g}$. Photoexcitation causes the net promotion of the lone $d_{x^2-y^2}$ electron to the d_{z^2} orbital. This creates the $^1A_{1g}$ state which, being an antibonding state, causes the temporary dissociation of the axial ligands. The subsequent decay of the $^1A_{1g}$ state to $^3B_{1g}$ and religation requires greater than 20 ns.[5,6]

Starting in the $^1A_{1g}$ state, upon photoexcitation, the nickel ion undergoes a net d–d transition ($d_{z^2}^2 \rightarrow d_{z^2}$, $d_{x^2-y^2}$) to form a B_{1g} state. Spectra obtained using low photon densities are representative of 4-coordinate ($^1A_{1g}$) nickel porphyrins. At high photon densities, new modes are observed that are at lower frequencies than the 4-coordinate ground state ($^1A_{1g}$) but higher than those observed for 5- and 6-coordinate complexes (see Table I). We attributed these new modes to an excited state which we have termed $^*B_{1g}$ to denote that the electron promotion has occurred to the $d_{x^2-y^2}$ orbital. The multiplicity of the $^*B_{1g}$ state is as yet undetermined; however, it is reasonable that the state will have a spin multiplicity of three.

It should be pointed out that the $^*B_{1g}$ state is favorably disposed toward the acquisition of axial ligands, such as nitrogenous bases.[3,4,15] Formation of a weak axial bond with solvent molecules could be a possible explanation for the $^*B_{1g}$ state reported here. Even H_2O can be a weak axial ligand for a nickel porphyrin under certain conditions.[16] However, we believe this is an unlikely explanation of our data because of the diversity of solvent conditions under which several different nickel porphyrins exhibit qualitatively similar photodynamics. For example, NiPPDME in anhydrous toluene exhibits the same excited-state behavior as

(15) Ake, R. L.; Gouterman, M. *Theor. Chim. Acta* **1970**, *17*, 408–416.

(16) Pasternack, R. E.; Spiro, E. G.; Teach, M. J. *Inorg. Nucl. Chem.* **1974**, *36*, 599–606.

that observed for NiPP in CTAB micelles. Small solvent dependences are observed but their nature and magnitude are not consistent with the formation of any type of weak axial ligand bond.

Power Dependence and Dynamics of the Excited State. The power dependence observed for the formation of the excited-state species, by using Q-band excitation (532 nm), shows a linear dependence on the square root of the incident laser power. We assume we are probing a state that has a lifetime of ≈250 ps, using a ≈10-ns-wide laser pulse.[3,4] The possibility of generation of an excited state by nonlinear processes exists especially at the relatively high photon densities required to generate $^*B_{1g}$. The power dependence observed indicates that this is not the case. The two-photon dependence of the $^*B_{1g}$ state arises from the requirement of one photon to generate the excited-state species and another to scatter from the state once it is formed. The high photon density requirements, therefore, are a result of the necessity that the two photons must arrive at the photoexcited molecule within ≈250 ps of each other (i.e., before the state formed by the first photon decays back to the ground state).

The extent to which the $^*B_{1g}$ excited state can be produced, by using a several-nanosecond-wide laser pulse, was explored by using a simple equation to model the excited-state population as a function of time during the laser pulse. The lifetime data obtained by Kim et al.[3,4] was used for the decay rate of the excited state, and excited-state populations were calculated by using a slightly modified version of an equation derived by Birge.[17] This equation models the population of the excited state, taking into consideration parameters such as laser power, excited-state lifetimes, excitation wavelength, pulse width, and absorptivity at the incident laser frequency. A term was added that linearly scales quantum yield for the formation of the excited state. This equation[27] is

$$^*N(t) = {}^*N_{t-\Delta t} + {}^{abs}N_{\Delta t}(t) - {}^{d^n}N_{\Delta t}(t)$$

where $^*N(t)$ represents the total excited-state population (in this case, the $^*B_{1g}$ state) at time t, $^*N_{t-\Delta t}$ is the excited-state population at the last calculation increment, $^{abs}N_{\Delta t}(t)$ is the amount of excited-state species created during the time increment Δt being calculated, and $^{d^n}N_{\Delta t}(t)$ represents the amount of excited-state species that has decayed in the time increment being calculated. The time increment Δt has to be much shorter than the lifetime of the excited state in order for these calculations to have significance.[17] In these calculations, several simplifying assumptions have been made. All incident photons in the laser pulse are considered to be available for generation of the excited state. Also, the formation constant of the excited state has been neglected and assumed to be instantaneous. This should not affect the calculations since the formation rate, as measured by Kim et al.,[3,4] is a factor of ~16 times shorter than the decay rate from the excited state. Also, the absorptivity has been approximated in these calculations to be ~15 000 M cm^{-1}, a reasonable value for the nickel porphyrins used in this study.

Figure 6 presents results of calculations where all parameters were held constant except the lifetime of the excited-state species. The results presented are of arbitrary intensity but allow comparison of the relative populations of the excited-state species present during the laser pulse with respect to different parameters in the calculation. An excited-state lifetime of 250 ps produces curve b in Figure 6. If this is qualitatively set to reflect the excited-state population observed in the spectra, it is apparent that the population of the excited-state species within the laser pulse is a linear function of the excited-state lifetime. Thus, an excited state with a lifetime of 50 ps would be very difficult to observe by using an 8-ns-wide laser pulse, while an excited-state species with a 500-ps lifetime would have stronger intensity than that of the state with a 250-ps lifetime. Also, shorter laser pulses with the same power per pulse produce a larger amount of excited-state

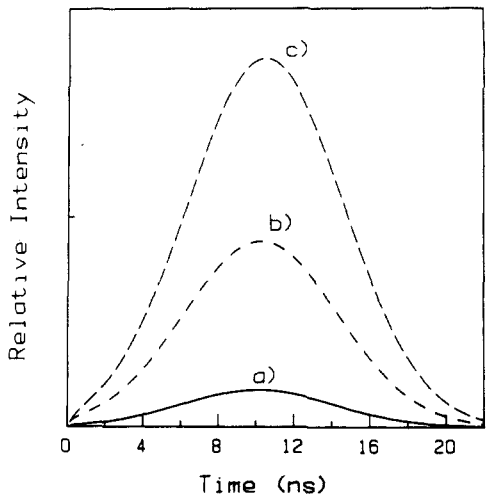

Figure 6. Plot of relative excited-state population as a function of time for several different excited-state lifetimes (τ). The laser pulse width was set to 8 ns for all calculations. All other parameters were held constant. Curve a represents excited-state population for an excited state with a lifetime of 50 ps, curve b for τ = 250 ps, and curve c for τ = 500 ps.

population (not shown), as one might expect on the basis of the increased photon density. Within this general model, an appreciable population of excited-state species is present during the relatively long laser pulse, allowing the detection of a species having subnanosecond lifetimes with nanosecond laser pulses. Similar results have recently been obtained for excited-state complexes of ruthenium bipyridine.[24]

Structural Properties of B^*_{1g}. Several modes in the porphyrin Raman spectrum have been correlated to changes in the distance between the pyrrole nitrogens and the center of the porphyrin.[18,19] These core size sensitive markers are prominent in the spectra of nickel porphyrins obtained with Soret excitation. Table II presents results of calculations of the core size from the frequency of $^4\nu_2$, $^4\nu_3$, and $^4\nu_{10}$ for 4-coordinate ground state, using the parameters determined by Choi et al.[20] As can be seen, the core size predicted for the 4-coordinate ground state by the frequencies of these modes agrees quite well and indicates a core size for the $^1A_{1g}$ state of ≈1.95 Å for NiPP, NiPPDME and NiOEP. The results of the same calculations, using marker line frequencies of the $^*B_{1g}$ state, indicate that the core has expanded to ≈2.01 Å to accommodate the added electron density in the metal $d_{x^2-y^2}$ orbital due to the promotion of one of the d_{z^2} electrons. This expansion appears necessary to lower the repulsion generated between this metal-centered d orbital and σ orbitals from the pyrrole nitrogens of the porphyrin macrocycle.

For the ground state of NiPP in pyrrolidine ($^3B_{1g}$) similar calculations using $^6\nu_3$ and $^6\nu_{10}$ indicate that the 6-coordinate ground state has a core size of ≈2.03 Å. Photoexcitation results in the formation of the $^1A_{1g}$ 4-coordinate ground state and is reflected in Raman shift positions of the new lines corresponding to $^4\nu_2$, $^4\nu_3$, and $^4\nu_{10}$. The core size of this new species is ≈1.95 Å, the same as that determined for the ground-state nickel porphyrins in noncoordinating solvents. The core size calculations of the $^*B_{1g}$ state, however, indicate a core size smaller than that observed for the equilibrium 6-coordinate complex.

The core size of the excited-state species ranges from ~2.01 to 2.02 Å, calculated from the positions of $^*\nu_3$ and $^*\nu_{10}$, and depends to some extent upon the solvent system (see below). The behavior of ν_2 in the 6-coordinate complex is similar to that observed in the $^*B_{1g}$ excited state in that it consistently indicates a substantially smaller core size than that calculated from the

(17) Birge, R. R. In *Ultra Sensitive Laser Spectroscopy*, Kliger, D. S., Ed.; Academic: New York, 1983; pp 109–175.

(18) Spiro, T. G. In *Iron Porphyrins*; Lever, A. B. P.; Gray, H. B., Eds.; Addison-Wesley: Reading, PA, 1983; Vol. 2, pp 89–160.

(19) Spaulding, L. D.; Chang, C. C.; Yu, N.-T.; Felton, R. H. *J. Am. Chem. Soc.* **1975**, *97*, 2517.

(20) Parthasarathi, N.; Hansen, C.; Yamaguchi, S.; Spiro, T. G. *J. Am. Chem. Soc.* **1987**, *109*, 3865.

positions of ν_3 and ν_{10}. This behavior also corroborates our evaluation of the character of the excited state. The consistency of this difference among the various nickel porphyrins in the wide number of noncoordinating solvents studied suggests that approximately two-thirds of the core expansion incurred in the transition from $^1A_{1g}$ to the ligated $^3B_{1g}$ state is due to the promotion of one of the d_{z^2} electrons. Therefore, the rest of the shift observed (core expansion) appears to result from ligation at the fifth and sixth axial sites.

A very approximate correlation of ν_4 to the movement of the core size markers (not shown) is observed and has a possible explanation in terms of the metal's interaction (or lack thereof) with the porphyrin π system. The position of ν_4 has been observed to shift with core size for the iron porphyrins where these correlations were first noted.[18-20] However, iron interacts with the porphyrin π system in a number of ways, including π backbonding. These complications are largely absent in nickel porphyrins.[15] Ignoring possible solvent effects (see below), it appears that the behavior observed in ν_4 of nickel porphyrins may reflect, in part, the sensitivity to changes in core size in a manner similar to ν_3. A recent study by Parthasarathi et al. has found this to be true for a variety of ground-state metalloporphyrins.[20]

Solvent Influence. A solvent effect on $^*B_{1g}$ was evident for all nickel porphyrins studied and was further characterized for NiPPDME. Nickel protoporphyrin dimethyl ester was the most convenient system because of its solubility in a variety of single-component noncoordinating solvents that have well-defined chemical properties. Solvent effects are seen in the vibrational properties of the NiPPDME in the $^*B_{1g}$ excited state and in the ground-state ($^1A_{1g}$) porphyrin absorption spectra. The former effect is most noticeable in the core size sensitive modes and ν_4. Interestingly, solvent effects upon the ground-state ($^1A_{1g}$) vibrational modes are either nonexistent or so small that they are not observable at the instrumental resolution of these experiments. A solvent-dependent shift of several wavenumbers has been detected in ν_4 (for the A_{1g} state) of nickel and copper tetra-*N*-methyl-4-pyridium porphyrin using the more sensitive Raman difference technique.[21]

Figure 4 illustrates the fact that the core size sensitive modes $^*\nu_2$, $^*\nu_3$, and $^*\nu_{10}$ display different solvent dependences for the $^*B_{1g}$ excited state: $^*\nu_3$ and $^*\nu_{10}$ exhibit a systematic dependence upon $E_T(30)$ while $^*\nu_2$ does not. Our results suggest a strong correlation between solvent $E_T(30)$ and the frequencies of several of the lines observed for the $^*B_{1g}$ state but little dependence for the vibrational modes of the 4-coordinate equilibrium species. Furthermore, the Raman spectra of the $^*B_{1g}$ state shows a correlated decrease in the frequencies of $^*\nu_{10}$ and $^*\nu_3$ with increasing $E_T(30)$ (as can be seen by comparison of the data in Tables I and II), while the frequency of $^*\nu_2$ does not show a systematic dependence on that parameter. A plot of solvent dipole moment (determined for the gas phase) vs $^*\nu_2$, $^*\nu_3$, and $^*\nu_{10}$ for solutions of NiPPDME reveals that only $^*\nu_3$ shows evidence of a systematic dependence. It appears, then, that more than one solvent property affects the excited state and that the $E_T(30)$ parameter best takes into account these multiple interactions.

The bands ν_3 and ν_{10} have been calculated to have appreciable contributions from the $\nu_{C\alpha-Cm}$ vibrational motion.[22] On the other hand, C_B–C_B and $C_{\beta\text{-substituent}}$ motions are the primary contributions to the ν_2 normal mode. The C_m position has been shown to have significant electron density contributions from the a_{2u} orbital of the porphyrin π system, while the C_β–C_β bond is most likely to be affected by changes in the porphyrin a_{1u} orbital.[14,23] Thus it appears that the porphyrin a_{2u} orbital displays a solvent dependence. Moreover, since this solvent influence is magnified when the nickel is in a $^*B_{1g}$ excited state, it is reasonable that a metal–solvent interaction may be the ultimate origin of the a_{2u} solvent dependence. If the solvent effect upon the a_{2u} orbital is mediated by the metal, the excited state ($d^1_{z^2}$, $d^1_{x^2-y^2}$) must interact more effectively (albeit indirectly via the σ-bonding orbital), with the porphyrin a_{2u} orbital, than the a_{1u}, producing a solvent-dependent distortion of the a_{2u} electron density distribution. This putative distortion is reasonable because the a_{2u} orbital has considerable electron density on the pyrrole nitrogen (and thus should be strongly affected by changes in core size and nitrogen–metal

TABLE III: Visible Absorption Band Positions for a Number of Nickel Porphyrins[a]

coordn no.	solvent	$E_T(30)$	Soret	wavelength, nm α	β	int(α/β)
		Ni(PP)				
6	pyrrolidine	NA	430	584	552	0.58
4	H_2O/acetone	NA	396	559	521	2.61
4	SDS	NA	388	562	526	2.46
4	CTAB	NA	400	563	524	3.1
4	NaOH/MeOH	NA	396	559	521	2.96
4	DMSO	45	400	560	522	2.65
		Ni(PPDME)				
6	piperidine	35.5	430	584	550	0.6
6	pyrrolidine	NA	430	586	549	0.64
4	H_2O/acetone	NA	397	559	522	2.93
4	CCl_4	32.5	402	562	525	3.10
4	toluene	33.9	402	562	524	3.37
4	benzene	34.5	402	561	524	3.1
4	THF	37.4	399	560	522	2.97
4	Br–benzene	37.5	402	561	523	2.94
4	Cl–benzene	37.5	403	562	525	2.98
4	$CHCl_3$	39.1	398	559	521	2.86
4	CH_2Cl_2	41.1	397	559	520	2.81
4	acetone	42.2	396	558	521	2.90
4	DMSO	45	400	559	522	2.63
4	acetonitrile	46.0	395	557	520	2.79
4	nitromethane	46.3	396	558	520	2.75
4	benzyl alcohol	50.8	402	562	524	3.11
4	ethanol	51.9	396	559	521	3.5
4	methanol	55.5	395	558	520	2.91
		Ni(OEP)				
4	toluene	33.9	394	553	516	3.40
4	CH_2Cl_2	41.1	394	550	512	2.31

[a] This work was performed on either a Perkin-Elmer 559/A or 330 absorption spectrometer with resolution of ±1 nm. All spectra were recorded with air as the reference. Blanks were run to ensure no background absorption of the cuvette influenced the absorption spectrum of the sample. For spectra recorded with the P-E 330 spectrometer, the spectra were transferred to an HP-9500 computer, where the spectrometer background performed was removed. Sample temperature was approximately RT (19–20 °C) for all spectra shown. NA means not available.

(21) Shelnutt, J. A., unpublished results.
(22) Abe, M.; Kitagawa, T.; Kyogoku, Y. *J. Chem. Phys.* **1978**, *69*, 4526–4534.
(23) Shelnutt, J. A.; Ortiz, V. *J. Phys. Chem.* **1985**, *89*, 4733–4739.
(24) Casewell, G.; Spiro, T. G. *Inorg. Chem.* **1987**, *26*, 18.
(25) The nomenclature used in this work follows Abe et al. with the following modification: $^n\nu_k$ where n refers to the ligation state of the species and k is the vibrational mode described by Abe et al.[22]
(26) The designations A_{1g}, A'_{1g}, and A''_{1g} are parameters of the four-orbital model described in ref 14 and are not to be confused with the $^1A_{1g}$ state of Ni–porphyrin.

(27) The equation used defines $^*N_{s-\Delta t}$ as the total excited-state population at the previously calculated time interval. $^{abs}N_{\Delta t}(t)$ represents the excited-state species generated during the given time interval being calculated and has the form

$$^{abs}N_{\Delta t}(t) = [P_0 \exp(-t^2/(0.60056\Gamma^2))\Delta t](1 - \exp(-\sigma_\lambda CL))$$

In this equation, P_0 is the laser power at maximum intensity, t is time (seconds), and Γ is the laser pulse width in nanoseconds. The second term (outside of the brackets) includes sample parameters such as σ, the one-photon cross section at wavelength λ, C, sample concentration (in molecules per cubic centimeter), and L, the sample cell path length (centimeters). $^{dn}N_{\Delta t}(t)$ represents the amount of excited-state species which decay during the calculated time increment Δt. In this work, this term is simply defined as

$$^{dn}N_{\Delta t}(t) = (\Delta t/\tau)^*N_{t-\Delta t}$$

Δt is again the calculation time increment, τ is the excited-state lifetime, and the last term is as defined above, the excited-state population at the last calculated time increment. Technically, this last value is iteratively generated, but this simplification allowed rapid calculation with minimum error.

bonding interactions) while the a_{1u} orbital has no charge density on the pyrrole nitrogens. The hypothesis that the solvent is mainly influencing the a_{2u} orbital via the metal–solvent interaction is strengthened by the observation that, in the equilibrium species, $^6\nu_2$ also predicts a smaller core size than do $^6\nu_3$ and $^6\nu_{10}$ analogous to the behavior observed for the $^*B_{1g}$ species. This implies that this a "generic" effect resulting from the promotion of one of the d_{z^2} electrons of the $^1A_{1g}$ state into the $d_{x^2-y^2}$ orbital of the B_{1g} state characteristic of both the equilibrium 6-coordinate and excited states. Moreover, the solvent dependence of the Raman modes reflects the increased sensitivity of these electron density shifts to environmental influences in the excited state.

The absorption spectral data of NiPPDME in a variety of noncoordinating solvents is summarized in Table III. While this work is primarily concerned with properties of the excited state of nickel porphyrins in noncoordinating solvents, we have found several correlations between the ground-state absorption spectra and solvent parameters. Figure 5 depicts the correlation of the α/β intensity ratio (Figure 5C), the average energy of the B and Q bands, and the difference in energy of the B and Q bands (Figure 5A) to the solvent $E_T(30)$.

The excited-state interactions for solvents with $E_T(30)$ values above approximately 47 have been described in terms of "aprotic" interactions with the betaine dye.[13] This description is not directly applicable to porphyrin excited-state interactions. One interesting note that might explain the behavior of the alcohols is that if the solvents are ordered by increasing $E_T(30)$, and their dielectric constants are listed as well, the solvent dielectric constant increases in a fashion that approximately mimics solvent $E_T(30)$ until benzyl alcohol. At that point, the solvent dielectric constant drops precipitously from ~35 for nitromethane to ~13 for benzyl alcohol and then it starts to increase again. This behavior may be indicative of a change in the dominant solvent–metalloporphyrin interaction from inductive to dipolar effects.

The results of absorption studies provide evidence supporting the proposition that the a_{2u} orbital is the molecular orbital most affected by the solvent. The plots of absorption spectral parameters vs solvent $E_T(30)$ indicate that definite trends exist in both the average energy and the splitting of the B and Q bands. In the four-orbital model developed by Gouterman, A'_{1g} is defined as $0.5(E_B + E_Q)$ while A_{1g} is defined as half the separation of the a_{1u} and a_{2u} orbitals.[14,23] A plot of A_{1g} vs solvent $E_T(30)$ indicates that the average energies of the B and Q transitions increase as a function of $E_T(30)$. This observation alone does not indicate a unique mechanism by which the shift occurs. For example, does the $e_g(\pi^*)$ orbital increase in energy, thereby causing the increase in A'_{1g}, or do the a_{1u} and/or a_{2u} orbitals decrease in energy, causing the increase in the π–π^* separation?

An indication of the origin of the A'_{1g} solvent dependence is found in the energy spacing of the B and Q(α) bands as a function of the solvent. The splitting of the B and Q bands is simply related to the energy difference between the a_{1u} and a_{2u} orbitals (assuming the two-electron term A''_{1g} is constant for a given porphyrin and metal).[14,23,25] In fact, $E_B - E_Q$ is just $2(A^2_{1g} + A'^2_{1g})^{1/2}$, where A''_{1g} is a constant. Therefore, if the energy difference between the Soret and α bands increases, then so must the a_{1u}–a_{2u} splitting. Figure 5 demonstrates that the $E_B - E_Q$ mimics the trend observed for A'_{1g}, indicating that the a_{1u}–a_{2u} splitting does increase. For example, if a_{1u} and a_{2u} are both stabilized by higher solvent $E_T(30)$, then the energy of the lower of the two, the a_{2u} orbital, must decrease to a larger extent as discussed above. It is interesting to note that if the $e_g(\pi)$ and $a_{1u}(\pi)$ levels are unaffected by solvent, then $\Delta A_{1g} = \Delta A'_{1g}$ and a decrease in the a_{2u} level alone predicts an increase in A_{1g} (and thus $E_B - E_Q$) and also the observed increase in A'_{1g}. Thus, the solvent-dependent excited-state vibrational properties and ground-state absorption properties can both be satisfactorily explained in terms of solvent perturbation of the porphyrin a_{2u} orbital.

Any attempt to explain the solvent dependencies observed in this work must address two fundamental questions. First, does the solvent dependence of the vibrational frequencies in the $^*B_{1g}$ state have the same origin as the solvent effect observed for the ground-state absorption spectra? Second, if so, why is the solvent effect not strongly manifested in the Raman spectra of the A_{1g} ground-state species? The porphyrin absorption spectrum directly reflects the ground-state orbital energies and solvent sensitivities of the a_{1u}, a_{2u}, and e_g^* levels. On the other hand, the $^*B_{1g}$ excited state is metal-centered with the porphyrin in its electronic ground state so that, to first order, the $e_g(\pi^*)$ orbital is not involved in the vibrational properties of the $^*B_{1g}$ state. Nonetheless, the Raman spectrum in the $^*B_{1g}$ state can still be influenced by solvent effects on the ground-state porphyrin π orbitals which are apparently accentuated by the metal d–d excited state. A common origin of these two solvent effects may lie in the porphyrin a_{2u} orbital as described above.

The second question is more difficult to answer, but the data presented in this study indicate little or no solvent dependence of the 4-coordinate equilibrium Raman data upon solvent. In actuality, the 4-coordinate equilibrium species may exhibit a solvent dependence, but it is below the resolution of our experimental conditions. Unpublished results[21] of a Raman difference study of nickel tetra(*N*-methyl-4-pyridyl)porphyrins indicate that the 4-coordinate equilibrium Raman line ν_4 shifts only 2 cm^{-1} for $E_T(30)$ values ranging from ~63 to 45. The pertinent question then becomes: why is the solvent effect so pronounced in the $^*B_{1g}$ excited-state species? Its answer lies in the mechanism of the solvent interaction.

Models of the solvent–porphyrin interaction mechanism must allow for the modulation of the ground-state porphyrin a_{2u} orbital by the solvent, as well as the magnified solvent dependence of macrocycle vibrations induced by the metal-centered $^*B_{1g}$ excited state. These criteria are satisfied if the focus of the solvent–porphyrin interaction is near the area of the Ni–N bond. Changes in the polarizability of the N–Ni bonds of the porphyrin induced by promotion of an electron into the metal $d_{x^2-y^2}$ orbital could then serve to modulate those interactions as well as differentially stabilize the porphyrin a_{1u}, a_{2u}, and e^*_g orbitals. This explanation is also pleasing because it is the core size that is primarily affected by the solvent.

Summary

Spectra of the excited-state species of 4-coordinate nickel porphyrins observed by using 10-ns photoexcitation are characteristic of a state with significant B_{1g} character. The core size sensitive lines indicate that the excited-state species has a greatly expanded core relative to the equilibrium 4-coordinate species. Thus, for nickel porphyrins, most of the core expansion observed in the equilibrium 5- and 6-coordinate complexes results from the nickel d electron promotion involved in the transition from the 4-coordinate ($^1A_{1g}$) state to the B_{1g} state. Solvent environment appears to have little effect upon the 4-coordinate ground-state vibrational properties of nickel porphyrins but has significant effects upon d–d excited-state vibrational properties, as evidenced by the dependence of the core size markers $^*\nu_2$, $^*\nu_3$, and $^*\nu_{10}$ on solvent $E_T(30)$. Solvent effects upon 4-coordinate ground-state electronic absorption properties are observed, however. An explanation which accounts for both effects is that noncoordinating solvent molecules in the solvation sphere can affect the porphyrin a_{2u} orbital energy via the polarizability of the pyrrole nitrogen–nickel bond and that these effects are more pronounced when the central metal is in a d–d excited state. The solvent effects are revealed by changes in the core size of the $^*B_{1g}$ excited state and the α–β intensity ratios of the 4-coordinate ground-state porphyrin absorption spectrum.

Acknowledgment. We gratefully acknowledge the support of the Associated Western Universities (to E.W.F.), the NIH (GM33330 to M.R.O.), the Petroleum Research Fund as administered by the American Chemical Society (to M.R.O.), Sandia National Laboratories (to E.W.F. and M.R.O.), the U.S. Department of Energy (DE-AC04-76DP00789 to J.A.S.), and the Gas Research Institute (5082-260-0767 to J.A.S.).

Registry No. NiPP, 15415-30-2; NiPPDME, 15304-70-8; NiOEP, 24803-99-4.